

4. SITE 1153¹

Shipboard Scientific Party²

PRINCIPAL RESULTS

Site 1153 is located on ~28-Ma seafloor of Zone A, ~225 km east of the eastern bounding transform of the Australian Antarctic Discordance and slightly east of the center of the residual depth anomaly. Limited SeaBeam mapping suggests that the seafloor in this region is characterized by a generally chaotic terrain with oblique lineaments likely to have been formed by rift propagation. The site lies in a wide (8–10 km), deep (~5600 m) graben containing >200 m sediment. This is the second site in a generally east-west transit designed to locate the Indian/Pacific mantle boundary across the northern part of our operational area.

Between 0 and 268 meters below seafloor (mbsf), we recovered seven wash cores. These contained dark brown pelagic clay overlying calcareous ooze. The thicknesses of these units and the extent to which the cores are continuous are unknown. At ~268 mbsf, ~20 cm of hard, lithified carbonate ooze overlies relatively fresh aphyric pillow basalts, some of which have variably altered glass rims. Only 1.8 m of basalt was recovered from 7.3 m basement penetration before the hole became unstable and was abandoned.

Two handpicked glasses and one whole-rock powder were analyzed on board. The glasses are relatively primitive, with 8.1–8.4 wt% MgO. The whole rock has significantly less MgO content (~6.5 wt%), with higher K₂O and Ba than the glasses but is otherwise similar in composition. These compositional differences cannot be explained by crystal fractionation and are likely the result of alteration of the whole-rock groundmass.

Because there is at least one intervening propagating rift, Site 1153 lavas cannot be directly related to the present-day segmentation of the Southeast Indian Ridge (SEIR). Both glasses plot significantly off the low-pressure crystal fractionation trends defined by 0- to 7-Ma Zone A lavas, and they appear to have been derived from a mantle source of

¹Examples of how to reference the whole or part of this volume.

²Shipboard Scientific Party addresses.

somewhat more fertile composition by generally similar extents of melting.

On the Ba vs. Zr/Ba diagram, Site 1153 lavas appear to be distinctly Pacific in character, indicating that Pacific mantle was present within the depth anomaly at this time.

OPERATIONS

Transit to Site 1153

We made the 130-nmi transit to Site 1153 at an average speed of 12 kt. At 1045 hr on 29 November, the vessel slowed to 6 kt, and we conducted a 3.5-kHz survey across the precruise survey line. As on the first survey, the data were reviewed to verify sediment cover over basement. The data showed that the sediment cover was more than sufficient to provide lateral support for the bottom-hole assembly (BHA).

Hole 1153A

When the survey was concluded, a beacon was dropped on the prospectus site Global Positioning System coordinates at 1200 hr. The corrected precision depth recorder (PDR) depth referenced to the dual elevator stool was 5592.4 m. A nine-collar BHA was made up of a new C-7 four-cone rotary bit, a mechanical bit release, a head sub, an outer core barrel, a top sub, a head sub, seven 8¼-in drill collars, one tapered drill collar, six 5½-in drill pipes, and one crossover sub. Although no logging was anticipated, the mechanical bit release was affixed to free the BHA should the drilling assembly become stuck at the bit.

Hole 1153A was spudded with the rotary core barrel at 2300 hr on 29 November. The bit tagged seafloor at 5592.4 m. The drill string was washed ahead with a core barrel in place to 267.6 mbsf, where basalt was contacted. During the process of washing ahead without coring, seven wash barrels were recovered from 26.9, 142.3, 151.9, 209.6, 233.4, 243.0, and 267.6 mbsf (Table T1). The last wash barrel recovered some basaltic rock, so we began rotary coring. We experienced unstable hole conditions while washing from 243 to 268 mbsf. This condition required redrilling the bottom of the washed interval. When the drill string was pulled back to 248 mbsf, the driller noted ~40,000 lb of drag at 253 mbsf.

Prior to initiating rotary coring, the core barrel was dressed with a Whirl-Pak bag containing fluorescent microspheres as a circulating fluid contamination tracer. Before coring could be initiated at 268 mbsf, the driller had to ream the hole again from 248 to 268 mbsf. The hole was then flushed with a sepiolite mud treatment. The interval 267.6–274.9 mbsf was cored, but the hole became unstable again as 7 m of fill was encountered after we recovered the core barrel. The poor downhole conditions suggested a low probability that the hole could be deepened further, so coring was terminated. The drill string was recovered; the bit cleared the seafloor at 1030 hr and cleared the rotary table at 1630 hr on 1 December. The vessel was under way to the next site by 1900 hr on 1 December.

T1. Coring summary, Site 1153, p. 20.

IGNEOUS PETROLOGY

Basalt recovered from Hole 1153A between 243.0 and 274.9 mbsf (1.77 m) was assigned to a single lithologic unit that consists of slightly altered, medium gray aphyric pillow basalt. Vesicles are rare (<1%) and small (<1 mm). Although generally spherical, some vesicles are elongated, especially in Section 187-1153A-8R-2. Microphenocrysts of acicular plagioclase as long as 2.5 mm can be seen in hand specimen throughout Section 187-1153A-8R-2 and in some places in Section 187-1153A-8R-1. Microphenocrysts of skeletal olivine <0.4 mm are also present. Glassy rinds and/or chilled pillow margins occur on ~20% of the 32 pieces. Glass thickness is generally <2 mm, except for Sample 187-1153A-8R-1 (Piece 14), which is predominantly glass and is 2 cm thick. Groundmass texture in the pillow margins varies from glassy to intersertal, indicating rapid cooling. Spherulites (~1.5 mm diameter) are visible in hand specimen and associated with glassy rinds (e.g., Section 187-1153A-8R-1 [Piece 13]) (Fig. F1). These quench textures are highlighted by the alteration of the groundmass to a mixture of smectite and Fe oxyhydroxides. The thin section taken from Sample 187-1153A-7W-4 (Piece 3) illustrates the appearance of plagioclase sheaf textures (e.g., Fig. F2) within the glassy rind, which grades into a spherulitic zone toward the exterior of the chilled margin. Microlites of “Chinese lantern” olivine are also commonly associated with the chilled margins. Assessing relative proportions of groundmass phases in the chilled margins is impossible because the groundmass is cryptocrystalline. Fractures present in ~80% of the core are typical of pillow basalts, generally being either parallel or orthogonal to the pillow rims. Many of the pieces recovered are bounded by fracture surfaces and have V-shaped forms as described in “Igneous Petrology,” p. 4, in the “Site 1152,” chapter.

ALTERATION

Slightly altered basalt was recovered throughout Hole 1153A. The degree of alteration differs from piece to piece and is more intense along margins and around fractures and vesicles. Approximately 70% of the vesicles are coated or filled by any or all of the following: cryptocrystalline silica, Fe oxyhydroxide, calcite, and rare zeolites (Section 187-1153A-8R-2 [Pieces 3 and 6]). The same alteration products are found as fracture fillings, again with the addition of carbonate material. Large (up to 0.8 cm) calcite-filled cavities occur in the lower half of Section 187-1153A-8R-2 (Fig. F3) and make up 2% of the rock. A single angular basalt fragment (Section 187-1153A-8R-1 [Piece 11]) is entirely covered by a 0.5-mm-thick layer of calcite (Fig. F4). Attached to this piece is a 2- to 3-cm-long strongly altered chilled (pillow?) margin in which small amounts of fresh glass are still preserved. Brown Fe oxyhydroxide entirely covers some fractures (e.g., Section 187-1153A-8R-1 [Piece 16B]) and extends for up to 10 mm around some fractures and up to 25 mm from the edges of pieces not cut by the drill (e.g., Section 187-1153A-8R-2 [Piece 2]). Fe oxyhydroxide frequently highlights igneous textures (e.g., the spherulitic plagioclase in Figs. F5 and F1). Small (1–2 mm) spots of Mn oxide are visible on fractured surfaces. In thin section, some groundmass olivine appears iddingsitized, whereas groundmass plagioclase is unaffected by alteration. A general overall decrease of Fe oxyhydroxide and smectite abundance toward the center of basalt frag-

F1. Spherulites in plane-polarized light, p. 9.



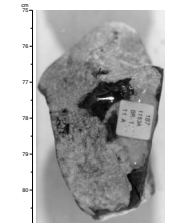
F2. Plagioclase sheaf texture with crossed polars, p. 10.



F3. Calcite-filled cavities in aphyric basalt, p. 11.



F4. Calcite-covered basalt fragment, p. 12.



F5. Fe oxyhydroxide highlighting spherulitic pillow margin, p. 13.



ments confirms the macroscopic observations, that the interior of the basalt fragments are least altered. Interstitial glass has been replaced by an opaque orange-brown material. Palagonite has replaced a large portion of most glassy rinds (e.g., Fig. F6). The degree of palagonitization is highest (~90%) on the outer layers of glass rinds (e.g., Section 187-1153A-8R-1 [Piece 5]) or in Section 187-1153A-8R-1 (Piece 14) at the center of a glass rind believed to mark the contact between two pillows. Palagonitization drops to <25% within a few millimeters and thereafter predominantly occurs along cracks. The centers of palagonite-filled cracks in Section 187-1153A-8R-1 (Piece 4) are occupied by silica veins, which are thickest (up to 1 mm) at the outer, most altered edges of the glass rind. The palagonite is symmetrically arranged around the silica, suggesting that the silica precipitated along an expanding crack after significant palagonitization had occurred. In Section 187-1153A-8R-1 (Piece 14), two thick (3 mm) calcite veins crosscut the center of a pillow rind (Fig. F7) and no silica can be observed under the binocular microscope, suggesting that different fluids have percolated through the lava pile. The most likely source for the calcite-bearing fluids is the carbonate overlying the basalt at Site 1153, whereas the cryptocrystalline silica may be derived from the hydrated glass. Whether these reflect temporal or local variations, however, is unknown.

MICROBIOLOGY

At Site 1153, one rock sample (Sample 187-1153A-8R-1 [Piece 15A, 106–109 cm]) and two sediment samples (Samples 187-1153A-4W-2, 92–97 cm, and 7W-3, 69–71 cm) were collected to characterize the microbial community (Table T2). The rock sample is a pillow basalt fragment including both the partly altered glassy margin and the more crystalline interior. The sediment samples consist mainly of clay and differ slightly in color from dark brown (Sample 187-1153A-4W-2, 92–97 cm) to grayish brown (Sample 187-1153A-7W-3, 69–71 cm). To minimize drilling-induced contamination, the outer surface of the rock sample was quickly flamed with an acetylene torch, and the sediment samples were collected from the centers of the cores. After the sterilization, enrichment cultures and samples for DNA analysis and electron microscope studies were prepared for each sample as described in “**Igneous Rocks**,” p. 7, in “Microbiology” in the “Explanatory Notes” chapter. Aliquots of a surface seawater sample were prepared for DNA analysis as described in “**Surface Seawater**,” p. 8, in “Microbiology” in the “Explanatory Notes” chapter.

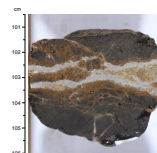
To examine the extent and type of contamination caused by drilling fluid, fluorescent microsphere tests were carried out for Cores 187-1153A-3W, 6W, and 8R (see “**Tracer Test**,” p. 9, in “Microbiology” in the “Explanatory Notes” chapter and Table T2). Smear slides from both outer and inner parts of the upper portions of the sediment cores were checked for microspheres under a fluorescence microscope, but none were detected in either the outer or inner smear slides. If the microsphere experiment had been successful, microspheres would be expected on the outer surface of the core. Because none were detected in this case, we conclude that they were flushed from the system and never reached this part of the core.

Pieces of rock from Core 187-1153A-8R were rinsed in nanopure water, the collected water was filtered, and the filters examined for the presence of microspheres under a fluorescence microscope. A thin sec-

F6. Palagonite and calcite veins in a fresh glassy pillow rind, p. 14.



F7. Calcite veins cutting through a glassy pillow margin, p. 15.



T2. Rock samples for cultures, DNA analysis, SEM/TEM, and contamination studies, p. 21.

tion from the inner part of the rock was also examined under a fluorescence microscope. Microspheres were observed on the filter but not in the thin section.

SITE GEOPHYSICS

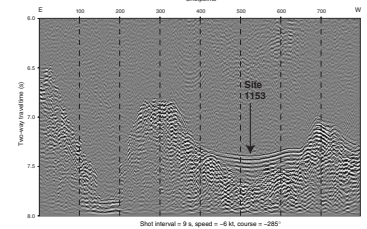
Site selection for Site 1153 was based on a single-channel seismic survey conducted during the *R/V Melville* cruise Sojourner 5 in 1997. The prospectus site is near shotpoint 520 of the seismic profile (Fig. F8). This migrated seismic profile shows clear sediment cover from 7.4 to 7.7 s two-way traveltime, giving an estimated sediment thickness of ~300 m. A 5-hr 3.5-kHz PDR survey was performed on approach to Site 1153 to verify the presence of sufficient sediment cover.

SEDIMENTS

Using precruise seismic surveys we estimated that the igneous basement at Site 1153 was buried under ~300 m of sediment. Our drilling strategy was to wash in the drill pipe and begin rotary coring once we contacted basement. Rather than wash down with a center bit, we opted to run a core barrel and retrieve it as required to ensure we recovered the uppermost basement. As a result, we recovered several cores that contained sediment from intervals significantly longer than the length of the core barrel. Because of the uncertainty in actual depth of the intervals sampled and the sediment core disturbance inherent in coring with a rotary bit, all sediment cores were designated as wash cores and given the core type notation of W. Since all of these cores had less than full core barrels, for curation purposes we adopted the same strategy as for hard rock cores, that is, shunting all the recovered material to the tops of sections. Despite the uncertainty and disturbance mentioned above, there is potential for valuable stratigraphic and paleontologic information to be gained from these cores.

Based mainly on composition, we subdivided the sediments recovered from this site into two units. Sedimentary Unit A (0 mbsf to between 233 and 243 mbsf) is a dark brown to very dark grayish brown clay. Some indistinct lighter-hued laminae are sporadically present, but several recovered intervals appear homogeneous. Trace phases in the sediments account for significantly <1% of the recovered core and include, in descending order of abundance, (1) subangular to subrounded brown translucent grains of volcanic glass (2–3 μm in size), (2) angular to prismatic or tabular grains of quartz and plagioclase of similar size, and (3) rare siliceous microfossils. Sedimentary Unit B (top: between 233 and 243 mbsf; bottom: between 243 and 267.6 mbsf) is a calcareous ooze that includes the same igneous trace phases as in sedimentary Unit A in similar abundances. The contact between these two units is sharp and marked by a 2-mm-thick coarse, sandy layer derived from a manganese crust. We cannot determine if the fragmentation of this crust was drilling induced, but there is a thin layer of fine calcareous sand just beneath it, suggesting it was recovered with little disturbance. Below the contact the color of the sediment gradationally changes color to light yellow brown over a short recovered interval. Throughout this gradational color change, the core also exhibits evidence of core disturbance as lighter-hued clay is marbled and mottled through a matrix of dark clay.

F8. Seismic profile crossing the Site 1153 location, p. 16.



Fortunately the contact between the units is reasonably well fixed, considering the nature of our drilling operation. Our strategy was to recover a core barrel whenever the driller noted a significant change in drilling conditions or penetration rate, with the hope of sampling the top of the igneous basement. Core 187-1153A-5W had been retrieved after washing down to 233 mbsf, but drilling conditions changed noticeably at about 243 mbsf, so the core barrel was retrieved. Thus, the wash barrel, which included the transition (Core 187-1153A-6W), only penetrated ~10 m from the bottom of the previous recovered interval. Therefore, the contact between carbonate-free sediment and calcareous ooze must lie between 233 and 243 mbsf, most likely near the bottom of that interval. The total thickness of carbonate sediment above the basaltic basement can be no more than ~30 m.

Considering the water depth of Site 1153 (>5700 m below sea level), we did not expect to see carbonate sediment overlying igneous basement. However, using the estimated age of the basement at this site from paleomagnetic data (~28 Ma) and the theoretical seafloor subsidence algorithm of Sclater et al. (1985), we can estimate that, at the time of formation, the depth below sea level of the igneous rocks recovered from Site 1152 was <4000 m, which is within the carbonate compensation depth range of the modern Indian Ocean.

GEOCHEMISTRY

Introduction

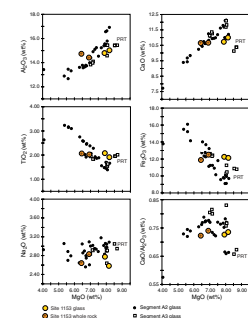
Site 1153 basalts were recovered from ~28-Ma seafloor formed within Zone A of the SEIR. One whole-rock powder was analyzed by both X-ray fluorescence (XRF) and inductively coupled plasma–atomic emission spectrometry (ICP-AES); two samples of fresh basalt glass chips were analyzed by ICP-AES only. The results are shown in Table T3. The whole-rock ICP-AES analyses are of poor quality because of dissolution problems and inexperience with the JY2000 instrument early in Leg 187. We reanalyzed the glass samples later in the leg, and both results are presented in Table T3. For the figures, only the averages of the rerun results are used. Note that, in the original analyses, SiO₂ content was estimated by difference from 100%. Otherwise, the original and rerun glass analyses agree very well for most elements and there were no systematic biases. Despite the analytical difficulties, XRF and ICP-AES analyses agree well, with the exception of Ni and Cr, which are both lower in the ICP-AES analyses, and Ba, which is below the detection limit of the XRF.

Hole 1153A

Samples from Hole 1153A are assigned to a single aphyric basalt unit, based on macroscopic and microscopic examination (see “Igneous Petrology,” p. 3). The single whole-rock sample analyzed contains ~6.5 wt% MgO (Fig. F9), ~0.2 wt% K₂O, and ~11 ppm Ba. As noted for Site 1152, the glass samples from Hole 1153A have higher MgO contents (8–8.4 wt%), lower K₂O contents (0.08–0.13 wt%), and lower Ba contents (5.2–8.5 ppm) than the associated whole rock (Table T3). All other elements are similar in both whole-rock and glass samples. The compositional differences between the whole-rock and the glass samples cannot result from simple low-pressure crystal fractionation, as the whole-rock glass tie lines are oblique to the fractionation trends for 0- to 7-Ma Zone

T3. Compositions of basalts from Site 1153, p. 22.

F9. Major element variations vs. MgO of Site 1153 basalts compared with young Zone A glasses, p. 17.



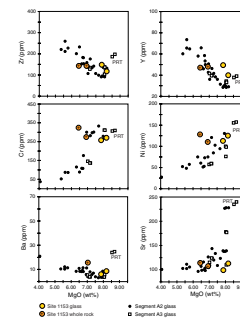
A lavas (Figs. F9, F10). These observations are similar to those from Site 1152, again suggesting that alteration or nonequilibrium magmatic processes have affected the whole-rock compositions.

Site 1153 glasses have higher Ti, Fe, Zr, Y, and Ba and lower CaO and Cr, compared with axial Zone A lavas of the same MgO content that are not associated with this propagating rift environment. The Site 1153 glasses are displaced from Zone A low-pressure crystal fractionation trends, away from the more evolved compositions typical of Zone A toward the distinct, more primitive, Zone A propagating rift tip (PRT) glass compositions (Figs. F9, F10). Higher Ti, Zr, Y, and Ba in the Site 1153 glasses and Zone A PRT lavas could result from either a more fertile mantle source or a lower degree of melting of the same mantle source. The low Na contents of Site 1153 glasses relative to 0- to 7-Ma Zone A axial glasses suggest a higher extent of melting, more than typical for PRT lavas from Zone A. High Fe_2O_3 in the Site 1153 glasses suggests a greater mean depth of melting. These compositional variations suggest that Site 1153 and PRT lavas have formed by slightly different degrees of melting, from a deeper, more fertile mantle source than most Zone A lavas. The similarity of Site 1153 and PRT lavas is not surprising, as Site 1153 is in one of a series of en echelon grabens that are likely associated with rift propagation.

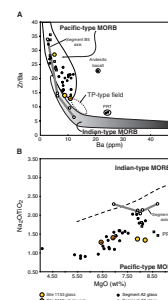
Mantle Domain

The Ba/Zr systematics of Site 1153 basalts suggest that Pacific-type mantle was present beneath Zone A at ~28 Ma (Fig. F11). The $\text{Na}_2\text{O}/\text{TiO}_2$ vs. MgO diagram is also consistent with a Pacific-type mantle. Because Site 1153 glasses have higher TiO_2 at a given MgO content, they plot at significantly lower $\text{Na}_2\text{O}/\text{TiO}_2$ than the 0- to 7-Ma Zone A glasses (Fig. F11B).

F10. Trace element variations vs. MgO of Hole 1153 basalts compared with young Zone A glasses, p. 18.



F11. Variations of Zr/Ba vs. Ba and $\text{Na}_2\text{O}/\text{TiO}_2$ vs. MgO from Site 1153, p. 19.



REFERENCE

Sclater, J.G., Meinke, L., Bennett, A., and Murphy, C., 1985. The depth of the ocean through the Neogene. *In* Kennett, J.P. (Ed.), *The Miocene Ocean: Paleooceanography and Biogeography*. Mem.—Geol. Soc. Am., 163:1–19.

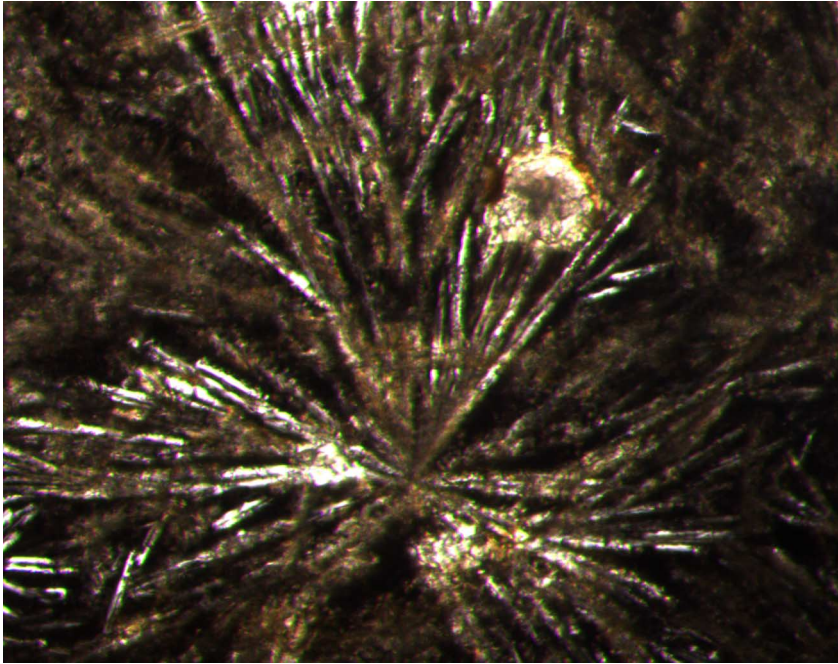
Figure F1. Photomicrograph in plane-polarized light of Sample 187-1153A-8R-1 (Piece 13, 95–98 cm; see “Site 1153 Thin Sections,” p. 11), showing plagioclase spherulites altered to Fe oxyhydroxide. Field of view = 10 mm.



8 mm



Figure F2. Photomicrograph, with crossed polars, of Sample 187-1153A-7W-4 (Piece 3, 46–49 cm; see “[Site 1153 Thin Sections](#),” p. 10), showing plagioclase sheath texture.



0.5 mm



Figure F3. Photograph of interval 187-1153A-8R-2, 42–50 cm, showing calcite-filled cavities in aphyric basalt.



Figure F4. Photograph of interval 187-1153A-8R-1, 75–81 cm, showing a calcite-covered basalt fragment.

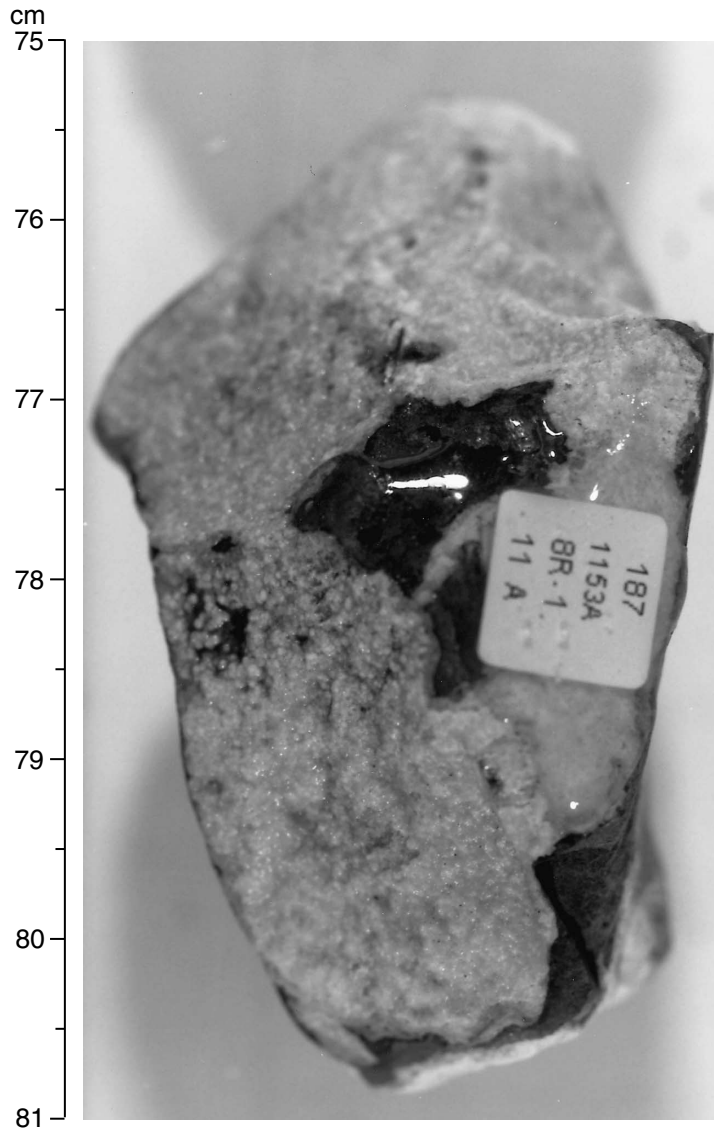


Figure F5. Photograph of interval 187-1153A-8R-1, 110–121 cm, showing a spherulitic pillow margin (outer edge at top) highlighted by Fe oxyhydroxide. Note: The photograph has been digitally enhanced.

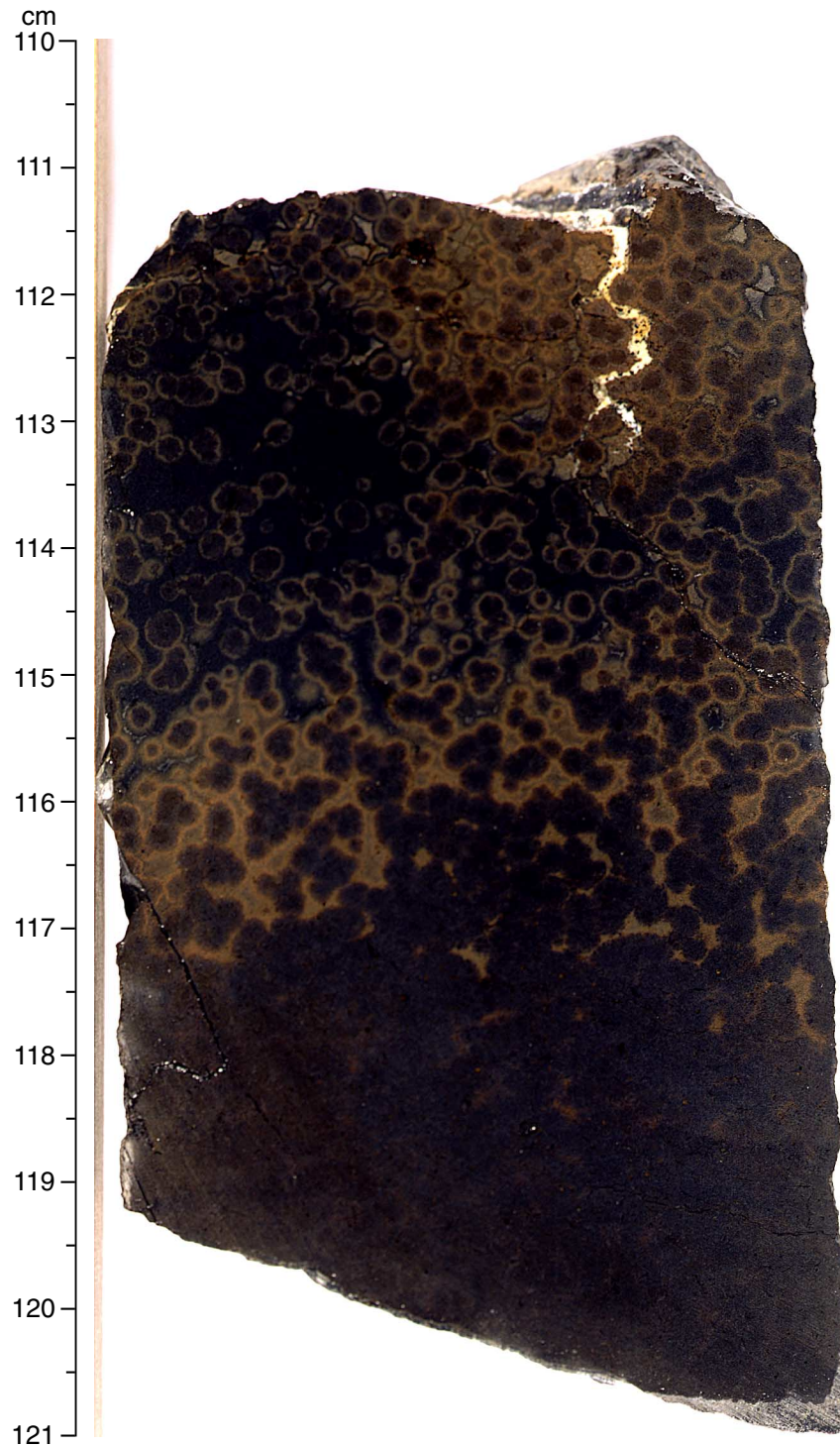


Figure F6. Photograph of Sample 187-1153A-8R-1, 101–106 cm, showing palagonite and calcite veins in a fresh glassy pillow rind.

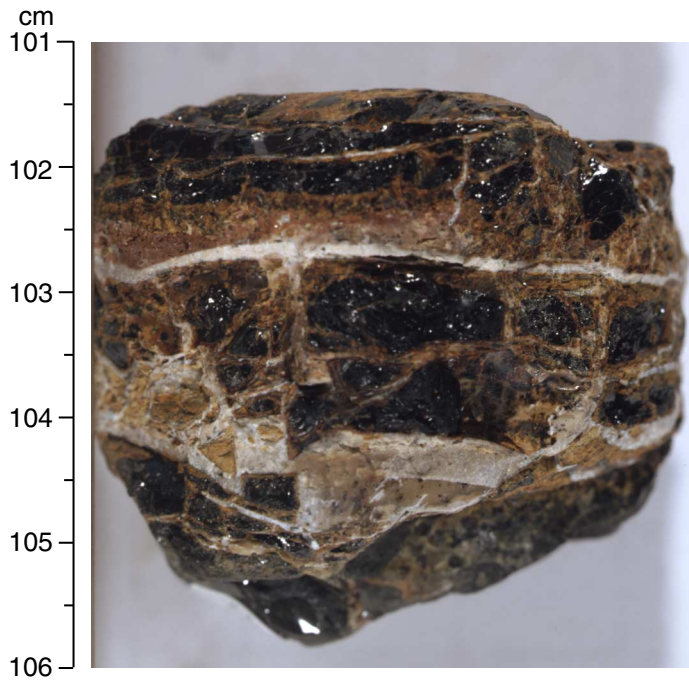


Figure F7. Photograph of Sample 187-1153A-8R-1, 101–106 cm (same piece as in Fig. F6, p. 14), showing calcite veins cutting through a glassy pillow margin.

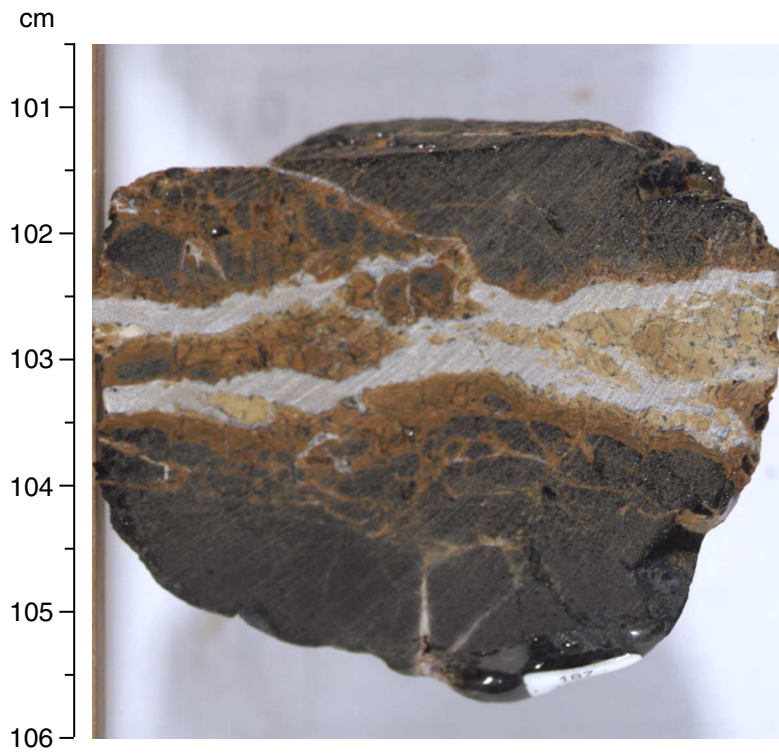


Figure F8. Seismic profile from *R/V Melville* cruise Sojourner 5 crossing the section of Site 1153. Shotpoints have been labeled every 15 min. Site 1153 is near shotpoint 520 (04:00–05:59 Universal Time Coordinated, 27 February 1997). Data have been filtered (1, 30, 375, 400), standardized, and migrated (90%).

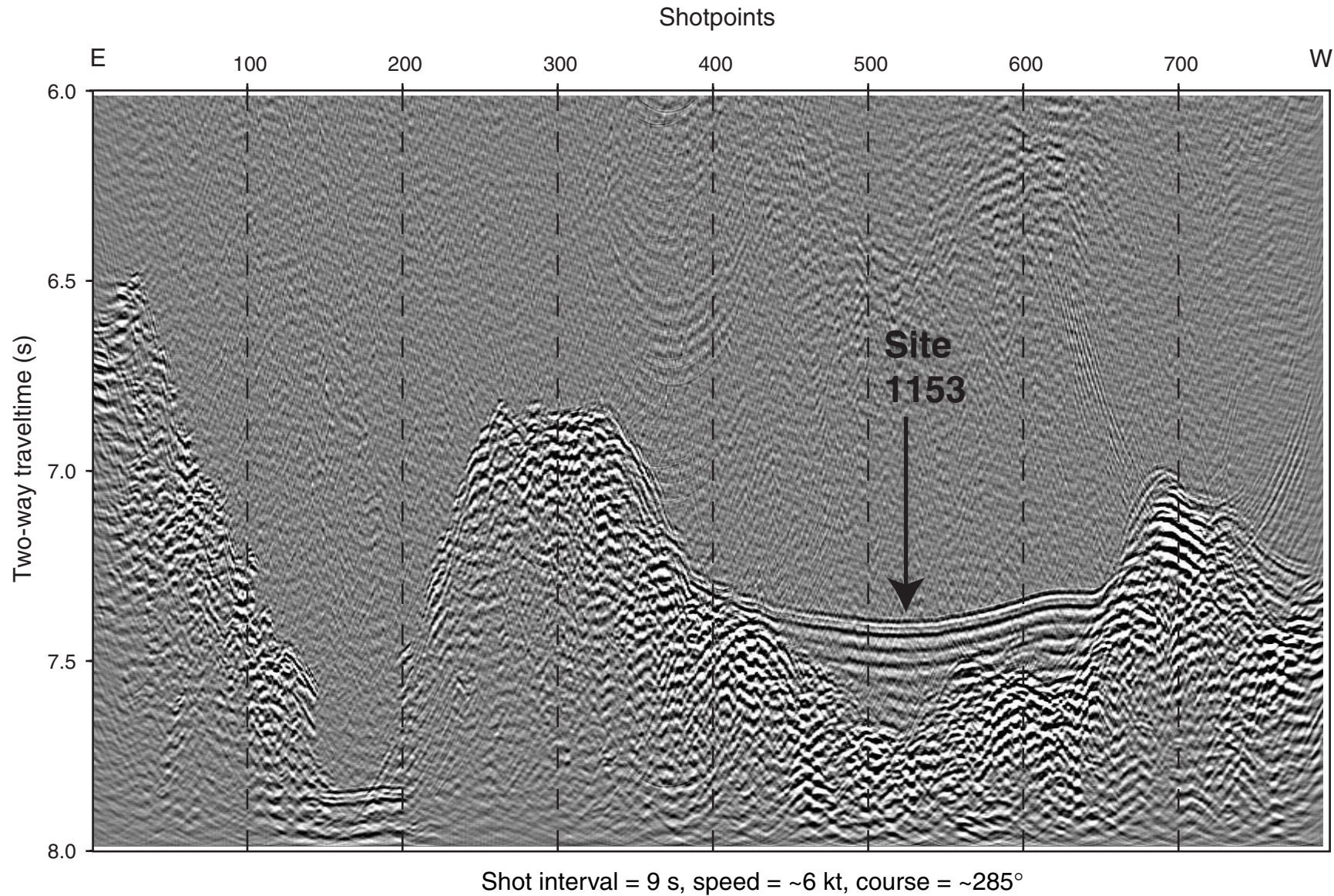


Figure F9. Major element variations vs. MgO of Site 1153 basalts compared with 0- to 7-Ma glasses from Zone A. PRT = propagating rift tip lavas from Segments A2 and A3. Only average X-ray fluorescence or average rerun ICP-AES values are shown.

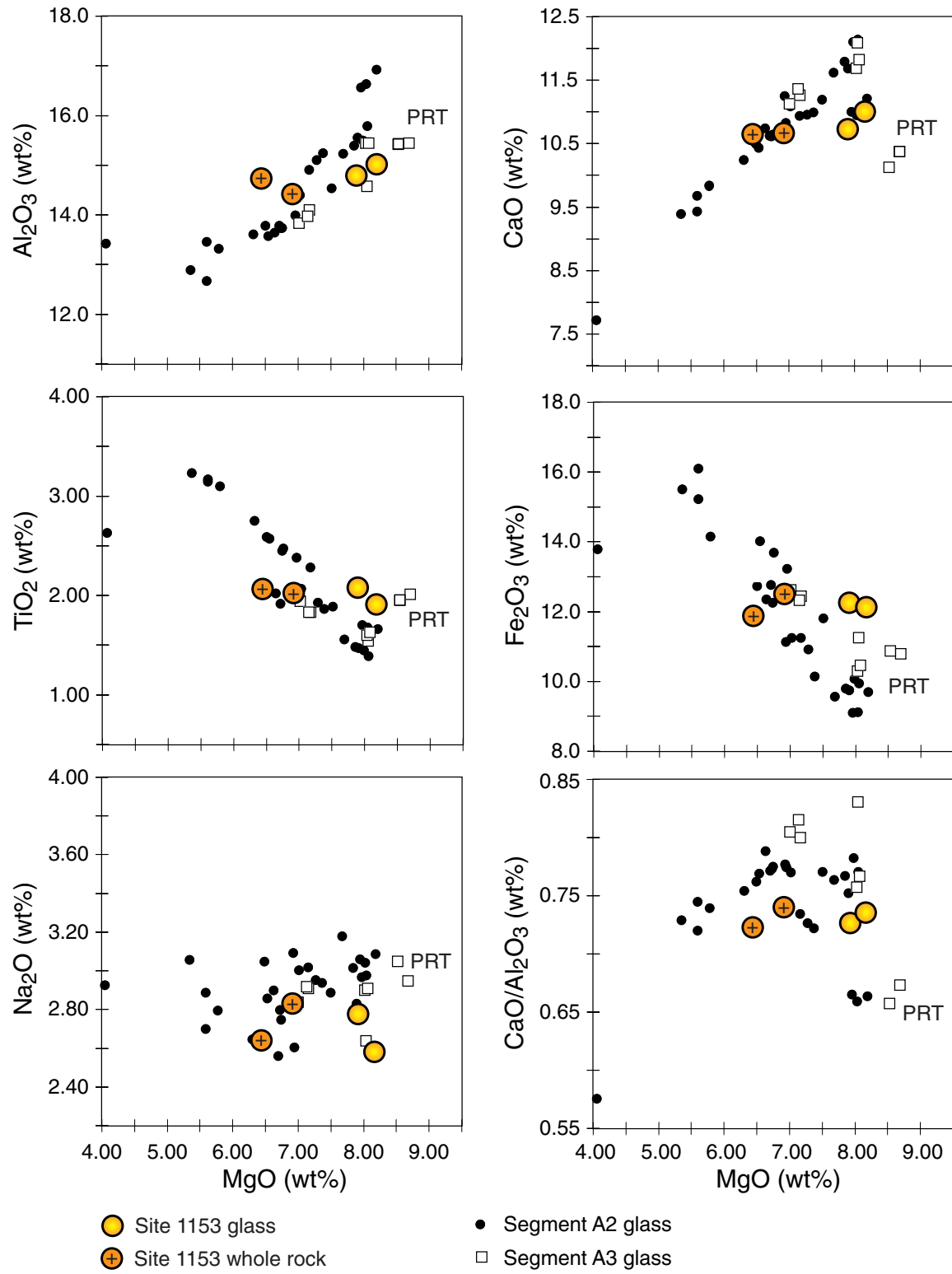


Figure F10. Trace element variations vs. MgO of Site 1153 basalts compared with 0- to 7-Ma glasses from Zone A. PRT = propagating rift tip lavas from Segments A2 and A3.

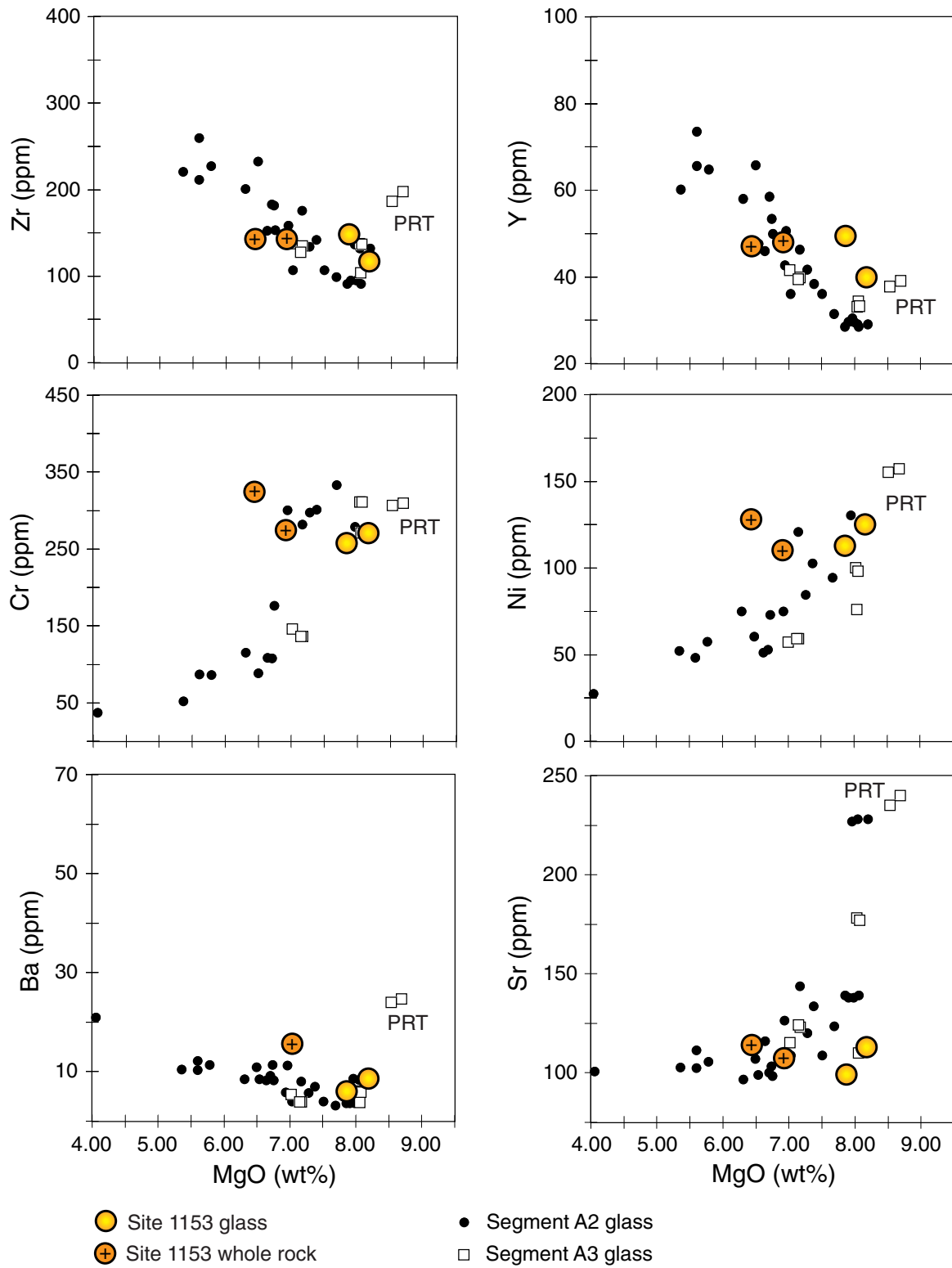


Figure F11. A. Variations of Zr/Ba vs. Ba for Site 1153 basaltic glass and whole-rock samples compared with Indian- and Pacific-type MORB fields defined by zero-age Southeast Indian Ridge (SEIR) lavas dredged between 123°E and 133°E. TP = Transitional Pacific; PRT = propagating rift tip lavas. B. A plot of Na₂O/TiO₂ vs. MgO of Site 1153 basaltic glass and whole-rock samples compared with Indian- and Pacific-type MORB fields defined by zero-age SEIR lavas dredged between 123°E and 133°E. The dashed line separates Indian- and Pacific-type zero-age SEIR basalt glass.

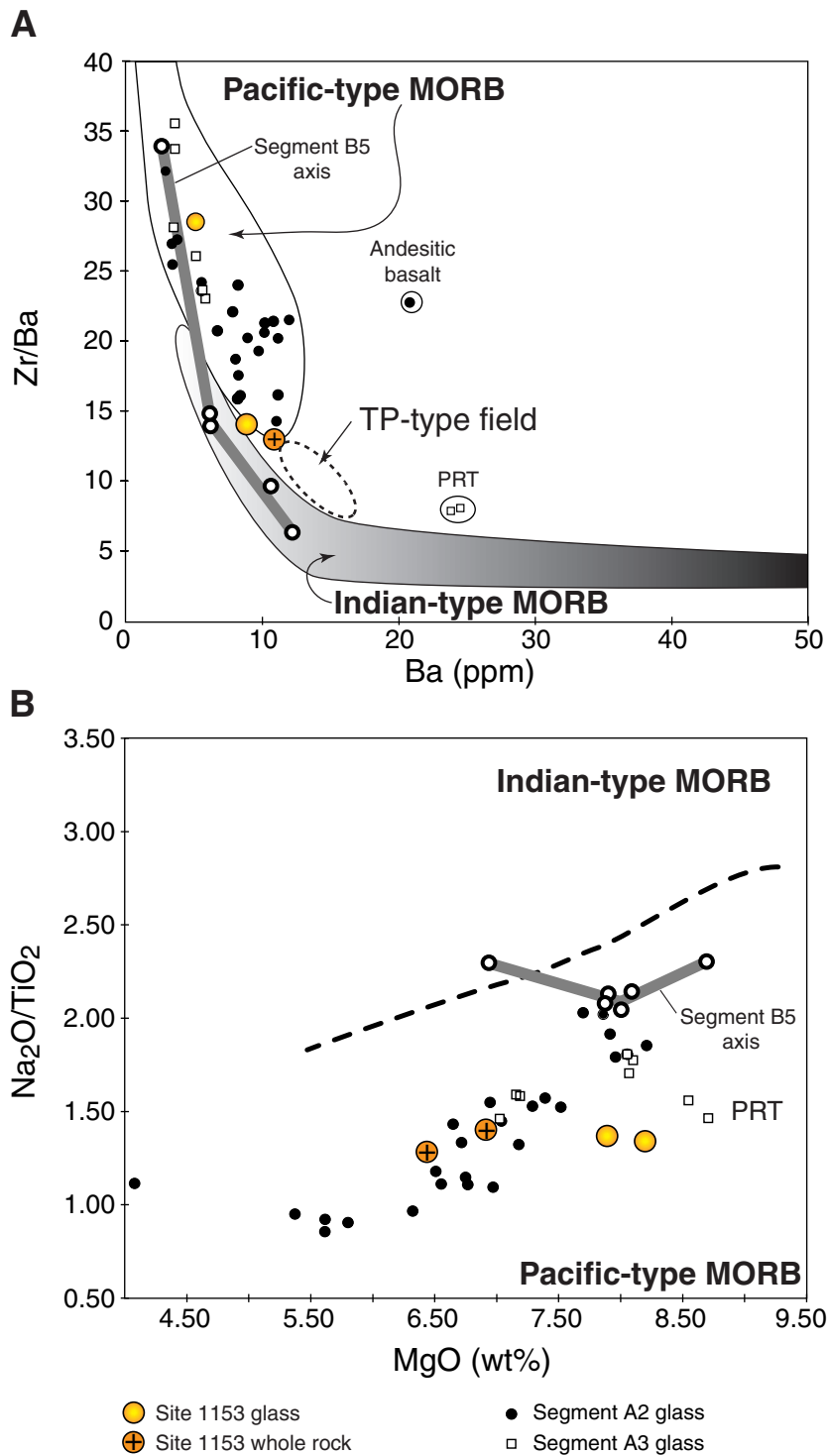


Table T1. Coring summary, Site 1153.

Hole 1153A

Latitude: 41°16.2914'S
 Longitude: 129°48.9085'E
 Time on hole: 1200 hr, 29 Nov 99–1900 hr, 1 Dec 99 (55.0 hr)
 Time on site: 1200 hr, 29 Nov 99–1900 hr, 1 Dec 99 (55.0 hr)
 Seafloor (drill-pipe measurement from rig floor, mbrf): 5592.4
 Distance between rig floor and sea level (m): 11.0
 Water depth (drill-pipe measurement from sea level, m): 5581.4
 Total depth (from rig floor, mbrf): 5867.3
 Total penetration (mbsf): 274.9
 Total length of cored section (m): 7.3
 Drilled interval (m): 267.4
 Total core recovered (m): 1.77
 Core recovery (%): 24.2
 Total number of cores: 8
 Number of drilled cores: 7

Core	Date (1999)	Ship local time	Depth (mbsf)		Length (m)		Recovery (%)	Comment
			Top	Bottom	Cored	Recovered		
187-1153A-								
1W	30 Nov	0100	0.0	26.9	26.9	0.00	N/A	
2W	30 Nov	0545	26.9	142.3	115.4	1.33	N/A	
3W	30 Nov	0745	142.3	151.9	9.6	4.72	N/A	Deployed Whirl-Pak on Core 3W
4W	30 Nov	1225	151.9	209.6	57.7	2.69	N/A	
5W	30 Nov	1600	209.6	233.4	23.8	4.35	N/A	
6W	30 Nov	1930	233.4	243.0	9.6	2.81	N/A	Deployed Whirl-Pak on Core 6W
7W	1 Dec	0500	243.0	267.6	24.6	4.53	N/A	First 23 cm curated as sediment. The rest of section curated as hard rock with Piece 1 beginning at 23 cm
8R	1 Dec	0915	267.6	274.9	7.3	1.77	24.2	Deployed Whirl-Pak on Core 8R
				Cored:	7.3	1.77	24.2	
				Drilled:	267.6			
				Total:	274.9			

Notes: N/A = not applicable. This table is also available in [ASCII](#) format.

Table T2. Rock samples incubated for enrichment cultures and prepared for DNA analysis and electron microscope studies and microspheres evaluated for contamination studies.

Core	Depth (mbsf)	Sample type	Enrichment cultures			DNA analysis			SEM/TEM samples		Microspheres†		
			Anaerobic	Aerobic	Microcosm*	Wash	Centrifuged	Fixed	Fixed	Air dried	Exterior	Interior	
187-1153A-													
3W	142.3-151.9	Sediment										No	No
4W	151.9-209.6	Sediment	9	3				X				No	No
6W	233.4-243.0	Sediment										No	No
7W	243.0-267.6	Sediment	10	3				X				No	No
8R	267.6-274.9	Rock	10	3	1 Mn	X		X	X	X		Yes	No
		Seawater					X	X					

Notes: * = microcosm for iron and sulfur or manganese (Mn) redox cycles; SEM = scanning electron microscope; TEM = transmission electron microscope; † = contamination test; X = sample prepared on board. This table is also available in [ASCII](#) format.

Table T3. Glass and whole-rock major and trace element compositions of basalts, Hole 1153A.

Core, section:	Hole 1153A									
	7W-4	7W-4	7W-4	7W-4	7W-4	7W-4	7W-4	8R-1	8R-1	8R-1
Interval (cm):	46-50	46-50	46-50	46-50	60-65	60-65	60-65	101-102	101-102	101-102
Depth (mbsf):	247.5	247.5	247.5	247.5	247.5	247.5	247.5	268.1	268.1	268.1
Piece:	3	3	3	3	5	5	5	14	14	14
Unit:	1	1	1	1	1	1	1	1	1	1
Analysis:	XRF	XRF	ICP	ICP	ICP	ICP, rerun	ICP, rerun	ICP	ICP, rerun	ICP, rerun
Rock type:	Aphyric basalt				Glass	Glass	Glass	Glass	Glass	Glass
Major element (wt%)										
SiO ₂	48.29	46.86	51.80	50.01	47.97*	51.41	52.30	46.90*	51.21	50.87
TiO ₂	2.08	2.05	2.08	1.97	2.07	2.09	2.06	1.93	1.94	1.96
Al ₂ O ₃	14.87	14.59	14.24	14.60	14.74	14.84	14.73	16.07	15.07	14.95
Fe ₂ O ₃	12.03	11.71	12.89	12.14	12.61	12.21	12.19	12.24	12.11	12.13
MnO	0.19	0.19	0.20	0.20	0.20	0.19	0.19	0.20	0.19	0.19
MgO	6.54	6.34	7.09	6.74	8.08	7.90	7.93	8.41	8.14	8.24
CaO	10.77	10.53	10.59	10.74	11.03	10.73	10.75	11.09	11.11	10.93
Na ₂ O	2.64	2.64	2.86	2.80	2.99	2.74	2.79	2.82	2.43	2.70
K ₂ O	0.22	0.22	0.18	0.19	0.11	0.09	0.08	0.13	0.13	0.13
P ₂ O ₅	0.20	0.19	0.22	0.22	0.20	0.17	0.19	0.22	0.16	0.18
LOI	0.89	0.89								
CO ₂										
H ₂ O										
Total:	98.72	96.21	102.16	99.61	100.00	102.35	103.22	100.00	102.50	102.29
Trace element (ppm)										
Nb	6									
Zr	143		144	142	171	153	146	133	109	124
Y	47		48	48	48	52	47	44	39	42
Sr	114		106	109	113	96	99	109	114	112
Rb	2									
Zn	104									
Cu	60									
Ni	128		111	109	118	108	117	121	132	119
Cr	324		269	280	270	261	265	287	276	270
V	355									
Ce	38									
Ba			11	11	8	5	5	8	9	8
Sc			38	40		40	39		32	36

Notes: Glass samples were rerun later in the course of Leg 187. Only the averages of these rerun analyses are plotted. * = SiO₂ by difference for ICP-AES; LOI = loss on ignition. This table is also available in [ASCII](#) format.